DOI: 10.1002/ejic.200700206

Influence of the Polypyridyl (pp) Ligand Size on the DNA Binding Properties, Cytotoxicity and Cellular Uptake of Organoruthenium(II) Complexes of the Type $[(\eta^6\text{-}C_6Me_6)Ru(L)(pp)]^{n+}$ [L = Cl, n = 1; L = $(NH_2)_2CS$, n = 2]

Sven Schäfer,[a] Ingo Ott,[b] Ronald Gust,[b] and William S. Sheldrick*[a]

Keywords: Ruthenium / Iridium / DNA / Antitumour agents / Arene ligands

The DNA binding of polypyridyl (pp) (η^6-hexamethylbenzene)ruthenium(II) complexes of the type $[(\eta^6\text{-}C_6Me_6)RuCl(pp)](CF_3SO_3)$ (pp = phen, tap, dpq, dppz, dppn) **1**–**5** and $[(\eta^6\text{-}C_6Me_6)Ru\{(NH_2)_2CS\}(pp)](CF_3SO_3)_2$ (pp = dpq, dppz, dppn) **6**–**8** has been studied by UV/Vis spectroscopy, circular dichroism and viscosity measurements. Complexes **3**–**5**, **7** and **8** are potent cytotoxic agents towards the human cancer cell lines MCF-7 and HT-29. Stable intercalative binding into CT DNA is indicated for the dpq and dppz complexes by large increases ΔT_m of 12–25 °C in the DNA thermal denaturation temperature for r = [complex]/[DNA] = 0.1. Large viscosity increases for DNA in the presence of **3** and **4** are also in accordance with this binding mode as are the pronounced hypochromic UV/Vis shifts for the π–π^* transitions of the dppz ligands of **4** and **7** in the range 360–400 nm. A small ΔT_m value of 2 °C and effectively unchanged viscosity suggest that Ru–N (nucleobase) coordinative binding is thermodynamically preferred for the larger polypyridyl ligand of **5** under equilibrium conditions, as is also the case for the small ligands phen and tap in complexes **1** and **2**. CD spectra indicate that the B DNA conformation is essentially retained for interaction with the chloro complexes **1**–**5** but that very significant distortions occur for the thiourea complexes **6**–**8**. The in vitro cytotoxicities of the chloro complexes **3**–**5** are dependent on the size of the polypyridyl ligand with IC_{50} values increasing in the order dppn < dppz < dpq: for instance IC_{50} values of 11.1, 2.12, and 0.13 μM were determined for **3**–**5** towards MCF-7. These values correlate well with the cellular uptake efficiency which increases from 1.1 over 146.6 to 906.7 ng(Ru)/mg (protein) within the series **3**–**5**.

Introduction

The intercalation of transition metal polypyridyl complexes into DNA has been a topic major bioinorganic interest in the past two decades and continues to receive much attention.[1–3] We have recently established that organometallic half-sandwich compounds of the types $[(\eta^5\text{-Cp*})Ir(amino\ acid\text{-}\kappa S)(dppz)]^{n+}$ (n = 1–3, dppz = dipyrido[3,2-*a*:2′,3′-*c*]phenazine)[4–6] and $[(\eta^6\text{-arene})Ru(amino\ acid\text{-}\kappa S)(dppz)]^{n+}$ (n = 1–3, arene = C_6H_6, $Me_3C_6H_3$, C_6Me_6),[7] with a thioether-coordinated methionine-containing amino acid or peptide, exhibit strong intercalative binding into DNA. In these complexes and in $[(\eta^5\text{-Cp*})Ru(dppz)(NO)](CF_3SO_3)_2$,[8] the magnitudes of the binding constants K_b (8.8×10^4 to 5.5×10^6 M^{-1}) are clearly dependent on the overall cation charge n (1–3), i.e. on additional electrostatic interactions with the negatively charged phosphodiester backbone of DNA.

This finding is in accordance with the results of Sartorius and Schneider[9] for heterocyclic derivatives with positively charged ammonium groups in their side chains. These authors also found that the intercalation binding strength is essentially a function of the size of the aromatic system, independent of heteroatoms or the presence of local positive charges within such planar moieties. Sterical considerations suggest that such a simple size dependence will be unlikely for the side-on intercalation mode (Figure 1) established by 2D-NOESY[7] for the interaction of $[(\eta^6\text{-}C_6Me_6)Ru(Ac\text{-}met\text{-}OH\text{-}\kappa S)(dppz)]^{2+}$ (Ac-met-OH = *N*-acetyl-L-methionine) with the hexanucleotide $d(GTCGAC)_2$. Inspection of Figure 1 indicates, for instance, that increasing the surface area and length of the polypyridyl ligand by replacing dppz with dppn (benzo[*i*]dipyrido[3,2-*a*:2′,3′-*c*]phenazine) might favour this type of intercalation by enabling additional stacking with the adenine and cytosine bases of the left-hand strand. On the other hand, inevitable close non-bonding contacts between atoms of the additional six-membered ring of dppn and DNA riboses could prevent a suitable alignment of the polypyridyl ligand.

To establish whether there is, indeed, an optimum polypyridyl ligand (pp) for side-on intercalation of $(\eta^6\text{-}C_6Me_6)Ru^{II}$ complexes, we have now studied the DNA binding

[a] Lehrstuhl für Analytische Chemie, Ruhr-Universität Bochum, 44780 Bochum
Fax: +49-234-3214420
E-mail: william.sheldrick@ruhr-uni-bochum.de
[b] Institut für Pharmazie, Freie Universität Berlin, Königin-Luise-Str. 2–4, 14195 Berlin
E-mail: ottingo@zedat.fu-berlin.de

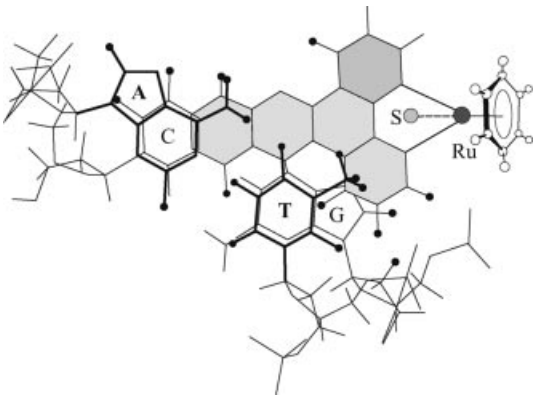

Figure 1. Schematic illustration of the side-on intercalation of [(η^6-C_6Me_6)Ru(Ac-met-OH-κ*S*)(dppz)]$^{2+}$ into the G_1T_2/C_6A_5 sequence of the hexanucleotide d(GTCGAC)$_2$.[7]

properties of compounds of the type [(η^6-C_6Me_6)RuCl(pp)]-(CF_3SO_3)$_2$ (**1**–**5**) with the diimine ligands phen (1,10-phenanthroline), tap (1,4,5,8-tetraazaphenanthrene), dpq (dipyrido[3,2-*f*:2′,3′-*h*]quinoxaline), dppz and dppn (Scheme 1). The preparation of [(η^6-C_6Me_6)RuCl(phen)]Cl has recently been reported by Süss–Fink et al.,[10] who studied the hydrolytic potential of the corresponding dicationic aqua complex [(η^6-C_6Me_6)Ru(H_2O)(phen)](BF_4)$_2$ for transfer hydrogenation reactions in aqueous solution. Both dppz and dppn have been confirmed as intercalating ligands in their Re^I complexes such as [*fac*-Re(CO)$_3$(pp)(pyridine)](CF_3SO_3),[11–13] which exhibit steric requirements similar to the half-sandwich polypyridyl (η^6-C_6Me_6)Ru^{II} complexes. As polypyridyl ligand intercalation and chloride substitution by purine nucleobases might be expected to compete as possible DNA binding modes for complexes **1**–**5**, three thiourea complexes [(η^6-C_6Me_6)Ru{(NH_2)$_2$CS}(pp)] (CF_3SO_3)$_2$ (pp = dpq, dppz, dppn) **6**–**8** were also investigated (Scheme 2). The *trans*-sited thiourea ligands in the metallointercalator [Pt(bpy){(NH_2)$_2$CS}$_2$]Cl_2 remain coordinated on DNA interaction and have been shown to play effectively no role in DNA binding.[14] As they are *cis*-sited relative to the polypyridyl ligands, additional N–H···O hydrogen bonding interactions to DNA could be possible for complexes **6**–**8**.

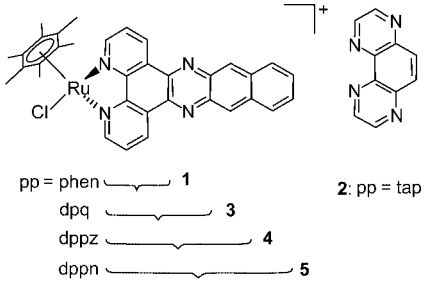

Scheme 1

Arene ruthenium(II) complexes have been shown to exhibit promising anticancer activity.[15,16] The first report appeared in 1990 when the amino acidato complex [(η^6-C_6H_6)-RuCl(L-H-Pro-O-κ^2*N*,*O*)] (H-Pro-OH = L-proline) was found to be significantly active in vivo towards mouse P388 leukaemia cells (T/C = 125% for a dosis 0.68 mg kg^{-1}) but inactive in vitro towards L1210 cells.[17] The in vitro cytotoxic properties of [(η^6-arene)Ru^{II}] complexes with phosphane,[16,21] sulfoxide[18–20] and chelating diamine or diimine ligands[15,22] have been investigated in recent years. Compounds of the latter type [(η^6-arene)RuCl(LL′)](PF_6) (LL′ = diamine or diimine) with extended polycyclic arenes (e.g. tetrahydroanthracene) and LL′ = ethylenediamine are most active towards A2780 human ovarian cancer cells, whereas those with polar substituents on the arene or with aromatic diimine ligands such as bpy or phen, exhibit considerably reduced activity.[23] As DNA is considered to be a possible target for (η^6-arene)Ru^{II} compounds,[15] we considered it to be of interest to also study the in vitro cytotoxity of complexes **3**–**5**, **7** and **8** with the extended polypyridyl ligands dpq, dppz and dppn, and to establish whether this can be correlated with the mode and strength of DNA binding and/or with cellular uptake. The human cell lines MCF-7 (breast cancer) and HT-29 (colon cancer) were selected for cytotoxicity studies.

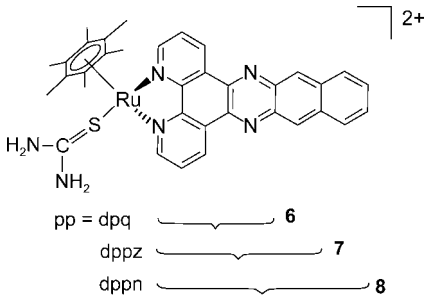

Scheme 2

Results and Discussion

Synthesis of 1–8 and Structures of 1 and 3

The compounds of the type [(η^6-C_6Me_6)RuCl(pp)]-(CF_3SO_3) **1**–**5** (pp = phen, tap, dpq, dppz, dppn) were prepared by refluxing the solvent complex [(η^6-C_6Me_6)-RuCl(acetone)$_2$] (CF_3SO_3) with the appropriate polypyridyl ligand (pp) in CH_3OH/CH_2Cl_2 for 2 h.

[(η^6-C_6Me_6)RuCl(acetone)$_2$]$^+$ can be obtained in situ by addition of two equivalents of Ag(CF_3SO_3) to a solution of the dimeric complex [{(C_6Me_6)$RuCl_2$}$_2$] in acetone and subsequent filtration of the precipitated AgCl after stirring in the dark for 0.5 h. Following removal of the remaining chloride ligand by analogous treatment of complexes **3**–**5** with a second equivalent of Ag(CF_3SO_3) in acetone, addition of thiourea to the resulting in situ complexes [(η^6-C_6Me_6)Ru(acetone)(pp)]$^{2+}$ affords [(η^6-C_6Me_6)Ru(pp)-{(NH_2)$_2$CS}] (CF_3SO_3)$_2$ **6**–**8** (pp = dpq, dppz, dppn) after refluxing the reaction mixture for 2 h in CH_3OH/CH_2Cl_2. All the complexes were characterised by ^{1}H and ^{13}C NMR

Table 1. Crystal and refinement data for **1** and **3**.

	1	**3**
Empirical formula	$C_{25}H_{26}ClF_3N_2O_3RuS$	$C_{26}H_{26}ClF_3N_4O_3RuS$
M	628.06	680.10
Measurement temperature [K]	293(2)	109(2)
Crystal system	monoclinic	monoclinic
Space group	$P2_1/c$	$P2_1/c$
a [Å]	8.9278(5)	14.3922(13)
b [Å]	11.5314(6)	11.6752(9)
c [Å]	24.0047(12)	15.4171(11)
β [°]	97.981(4)	96.469(7)
V [Å^3]	2447.3(2)	2574.1(4)
Z	4	4
F(000)	1272.0	1376.0
$\rho_{calcd.}$ [g/cm^{-3}]	1.705	1.755
Crystal size [mm]	$0.22 \times 0.13 \times 0.04$	$0.17 \times 0.10 \times 0.02$
Radiation	Mo-K_α	Mo-K_α
μ [mm^{-1}]	0.890	0.856
$2\theta_{max}$ [°]	25.0	27.5
h,k,l ranges	–10/10, –13/13, –28/28	–18/18, –15/15, –20/20
Collected reflections	30680	36744
Unique reflections	4298	5875
Observed reflections [$I > 2\sigma(I)$]	3992	3795
R_1 [$I > 2\sigma(I)$]	0.048	0.051
wR_2 [all data]	0.080	0.094
S (goodness-of-fit)	1.154	1.045
max./min. $\Delta\rho$(e Å^{-3})	0.72/–0.74	0.92/–0.98

and positive-ion LSIMS and gave satisfactory microanalyses. The structures of complexes **1** and **3** were determined by X-ray structural analysis (Table 1) and their respective cations are depicted in Figures 2 and 3. Complex **1** exhibits an interplanar angle of 54.1° between its benzene and polypyridyl ring systems, complex **2** a much larger angle of 75.2°. The individual $[(\eta^6\text{-}C_6Me_6)RuCl(pp)]^+$ cations pack with parallel polypyridyl ligands in their respective lattices.

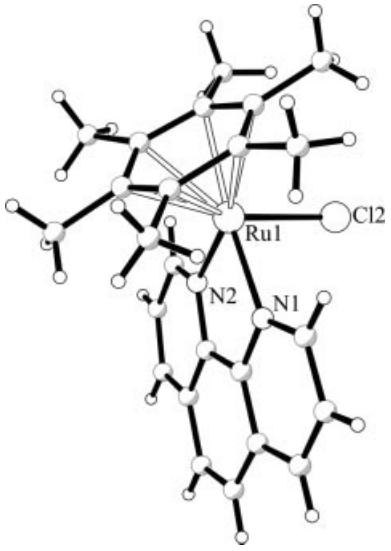

Figure 2. Molecular structure of the cations of $[(\eta^6\text{-}C_6Me_6)RuCl(phen)](CF_3SO_3)$ (**1**). Selected bond lengths [Å] and angles [°]: Ru1–Cl2 2.401(1) Ru1–N1 2.107(3), Ru1–N2 2.098(3), Ru1–C 2.194(3) – 2.251(3), N1–Ru1–N2 77.7(1), N1–Ru1–Cl2 85.08(8) N2–Ru1–Cl2 84.71(8).

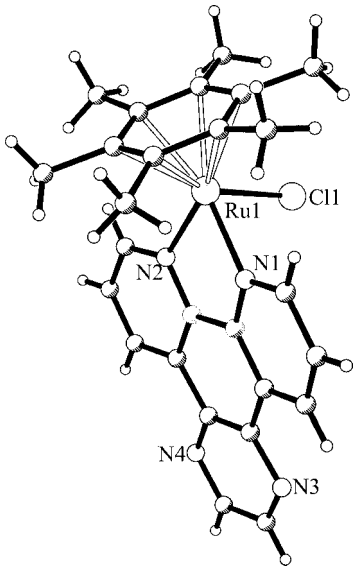

Figure 3. Molecular structure of the cations of $[(\eta^6\text{-}C_6Me_6)RuCl(dpq)](CF_3SO_3)$ (**3**). Selected bond lengths [Å] and angles [°]: Ru1–Cl1 2.408(1) Ru1–N1 2.109(4), Ru1–N2 2.101(4), Ru1–C 2.192(2) – 2.204(2), N1–Ru1–N2 77.1(1), N1–Ru1–Cl1 82.9(1) N2–Ru1–Cl1 84.7(1).

DNA Binding Studies

UV/Vis Absorption and Thermal Denaturation Studies for 1–8

Following an incubation period of 5 min, UV/Vis spectra for the buffered solutions of **1**–**4**, **6** and **7** (pH 7.2, 10 mM phosphate) with CT DNA at $r = 0.1$ {r = [complex]/[DNA] with DNA concentration in mol/L (nucleotide)} exhibit no

further significant changes, thereby indicating that achievement of equilibrium conditions is relatively rapid. A pronounced decrease in absorbance at about 364 and 383 nm and bathochromic shifts of about 5 nm are indicative of possible dppz intercalation into the biopolymer for complexes **4** and **7**. The time dependence of these changes is illustrated for the chloro complex **4** in part a of Figure 4.

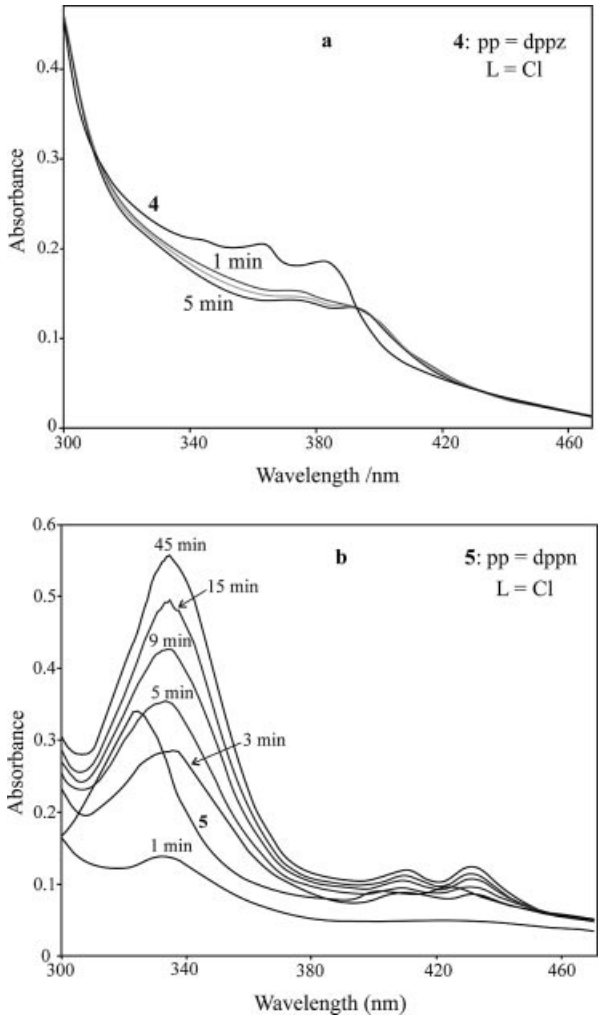

Figure 4. Time dependence of the UV/Vis spectra of complexes **4** and **5** (both 20 μM) in a 10 mM phosphate buffer (pH = 7.2) with CT DNA (200 μM). Times are given in minutes for individual curves.

Hypochromic shifts $\Delta A/A$ of respectively –28% and –16% at 364 nm are observed for **4** and **7** and indicate that the nature of the DNA interaction must be similar for both the dppz complexes. On mixing with CT DNA, the UV/Vis spectrum of the dppn complex **5** initially exhibits even more pronounced hypo- and bathochromic shifts for the spin-allowed π–π* transitions at about 327, 403 and 425 nm. Part b of Figure 4 depicts the $\Delta A/A$ value of –59% at 336 nm and the associated red shift of about 9 nm after 1 min. These initial spectral changes are followed by an increase in the absorbance values over the next 45 min to reach a maximum value of +63% at 336 nm. The original absorbance values of the complex are reached within 5 min after mixing. In similarity to complex **5** (Figure 4, b), significant decreases in $\Delta A/A$ are also observed for the dppn complex **8** at 327, 403 and 425 nm on initial mixing with DNA and these are followed by large increases with equilibrium being achieved within 15 min. The respective initial and final values of $\Delta A/A$ at the first maximum are –29% and +49%. No effective changes in absorption in the range 300–420 nm were recorded for the complexes **1** (pp = phen), **2** (pp = tap) and **3** (pp = dpq) on mixing with CT DNA. The UV/Vis spectra for all complex/[DNA] reaction mixtures exhibit no significant changes over a period of 36 h after equilibrium is achieved.

Thermal denaturation studies for CT DNA can provide simple a means of gauging the efficacy of polypyridyl intercalation for organometallic complexes[4–7] such as **1**–**8**, provided that electrostatic and hydrogen-bonding interactions with the biopolymer may be regarded as remaining effectively unchanged by pp ligand variation. The ΔT_m values listed in Table 2 for the monocations of **1**–**5** and the dications of **6**–**8** were recorded under equilibrium conditions in a phosphate buffer, (pH = 7.2) for $r = 0.1$ and are indicative of strong DNA intercalation for the dppz ligand of **4** (ΔT_m = 20 °C), and **7** (ΔT_m = 25 °C). In contrast, the DNA melting temperature remains effectively unchanged on treatment with complexes **1**, **2** and **5** [ΔT_m = 0 (phen), +2 (tap), +2 °C (dppn)]. A similar ΔT_m value of –2 °C has also been reported for $[(\eta^6\text{-}C_6H_6)RuCl(en)]^+$ (en = ethylenediamine),[22] which preferentially coordinates DNA guanine nucleobases at their endocyclic nitrogen atoms N7. The small ΔT_m value of only + 2 °C is more surprising for the larger dppn ligand with its much more extensive aromatic surface area, but in accordance with the previously discussed UV/Vis studies (Figure 4, b), which indicate an absence of dppn intercalation under equilibrium conditions. Relatively large increases in T_m of 14° and 12 °C are, however, observed for the dpq complexes **3** and **6** respectively, suggesting that this polypyridyl ligand could also participate in intercalative DNA binding. The significant increase in ΔT_m for the dicationic complexes **7** and **8** [ΔT_m changes: +5 (dppz), +6 °C (dppn)] in comparison to the monocationic species **4** and **5** may be caused by the increased strength of the electrostatic interactions with the biopolymer but the possibility of N–H···X (X = O, N) hydrogen bonding involving the thiourea

Table 2. Melting temperature shifts ΔT_m, for the interaction of complexes $[(\eta^6\text{-}C_6Me_6)Ru(L)(pp)]^{n+}$ (n = 1, 2) **1**–**8** with CT DNA ($r = 0.1$) in a 10 mM phosphate buffer at pH = 7.2 after incubation for 60 min.

Complex	pp	L		ΔT_m[°C]
1	phen	Cl	1	0
2	tap	Cl	1	2
3	dpq	Cl[a]	1	14
4	dppz	Cl[a]	1	20
5	dppn	Cl	1	2
6	dpq	$(NH_2)_2CS$	2	12
7	dppz	$(NH_2)_2CS$	2	25
8	dppn	$(NH_2)_2CS$	2	8

[a] Aquation can lead to the dications $[(\eta^6\text{-}C_6Me_6)Ru(H_2O)(pp)]^{2+}$ as intercalating species after incubation (pp = dpq, dppz).

amino functions and DNA acceptor atoms X cannot be ruled out. Interestingly a small relative decrease in ΔT_m of –2 °C is observed for the dicationic dpq complex **6** in comparison to its chloro analogue **3**.

Circular Dichroism Studies for 1–8

The high ΔT_m values recorded for the dppz complexes **4** and **7** in comparison to the dppn complexes **5** and **8** suggest that dppz may offer a close to optimum aromatic surface area for side-on intercalation into B DNA[7] (Figure 1) and that dppn may be too long and its surface area too extensive for effective DNA binding in this mode. Characteristic changes in the observed circular dichroism (CD) spectra of DNA provide a convenient means of monitoring conformational changes for the biopolymer.[7,24,25] As depicted in Figure 5, a negative band at 246 nm caused by the helical B conformation and a positive band at 275 nm due to base stacking are observed for CT DNA.[26] Addition of the phen and tap complexes **1** and **2** at a 1:10 complex/[DNA] molar ratio leads to only minor spectral changes, thereby indicating little distortion of the B helix following the formation of Ru–N bonds to DNA nucleobases. The spectra of Figure 5 and the CD spectra for the other complexes exhibited no significant changes during a period of 36 h following equilibrium achievement. Complex/[DNA] solutions remained clear and opalescence was not observed. The depicted spectra were all recorded after 24 h.

Although aromatic molecules often generate CD bands between 300 and 400 nm on interaction with DNA, the appearance of these signals is generally not of relevance for the assignment of the binding mode. This is because the observed induced circular dichroism is caused by a rigid orientation of the molecule with respect to the double helix and this can result from surface or groove binding in addition to intercalation. The dppz complexes **4** and **7** do, however, exhibit characteristic negative CD bands with molar elipticities [θ] of -4.1×10^{-3} and -1.9×0^{-3} deg cm^2 mol^{-1} at λ = 300 nm (Figure 6) and we have previously established[6] that the appearance of such bands in the range 290–340 nm is, indeed characteristic for intercalating organometallic dppz complexes. The observed wavelength range corresponds with that of the broad π–π* absorption maximum at λ_{max} = 280 nm of the complexes themselves. A small but significant increase in [θ] for the positive CD band at 272 nm for **4** may be attributed to additional stabilisation of base stacking in the helix due to dppz intercalation. Whereas the molar ellipticity for the positive band at 268 nm is also similar for the analogous thiourea complex **7**, a dramatic decrease in the negative value of [θ] for the band at 243 nm is apparent in the latter case. This implies a significant change in the original B helical conformation due possibly to both the twofold positive charge and the participation of thiourea amino functions in hydrogen bonding to the biopolymer.

The CD spectra for 1:10 mixtures of the dpq complexes **3** and **6** with CT DNA (Figure 7) also provide evidence for intercalation. When compared to the CD spectrum of CT DNA alone, a broadening and apparent splitting of the positive CD band are ascertainable for the **3**/DNA mixture and, to a lesser extent, the **6**/DNA mixture. As complexes **3** and **6** exhibit absorption maxima for spin-allowed MLCT π–π* transitions at λ_{max} 261 and 284 nm, the appearance of the positive band in the range 270–295 nm could be due to a spectral overlap with a negative CD contribution due to intercalating dpq ligands. This interpretation would correlate with the large ΔT_m values of 14 and 12 °C registered for these dpq complexes. The decrease in the negative value of the molar ellipticity [θ] for the band at 243 nm is less pronounced for **6** than for the analogous dppz complex **7**, but once again indicates that significant changes in the B DNA conformation must have taken place.

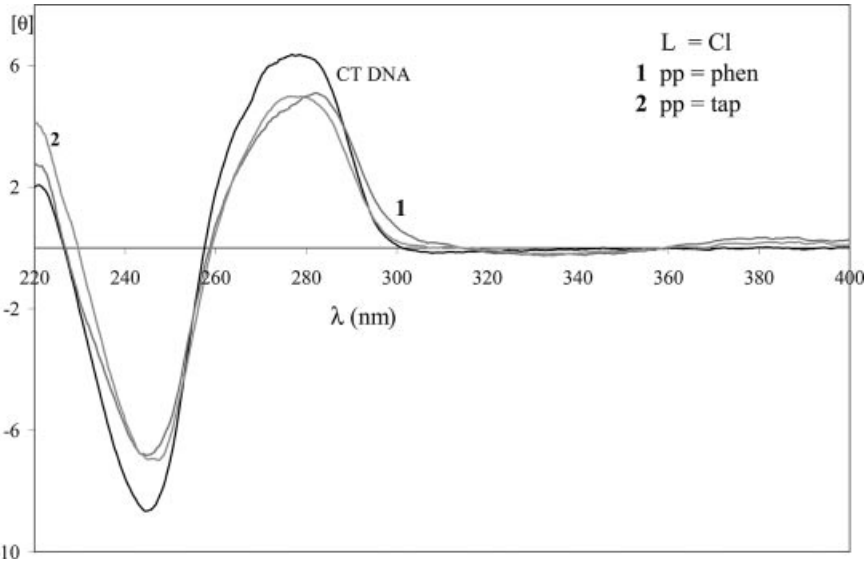

Figure 5. CD spectra of CT DNA and mixtures of **1** (pp = phen) and **2** (pp = tap) with CT DNA (r = 0.1) in a 10 mM phosphate buffer (pH = 7.2) after 24 h incubation.

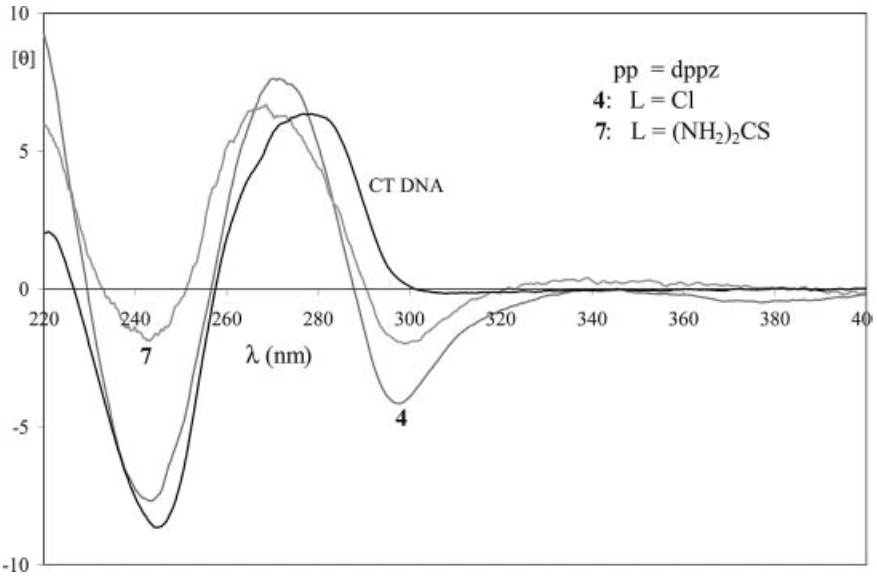

Figure 6. CD spectra of CT DNA and mixtures of **4** and **7** (pp = dppz) with CT DNA (r = 0.1) in a 10 mM phosphate buffer (pH = 7.2) after 24 h incubation.

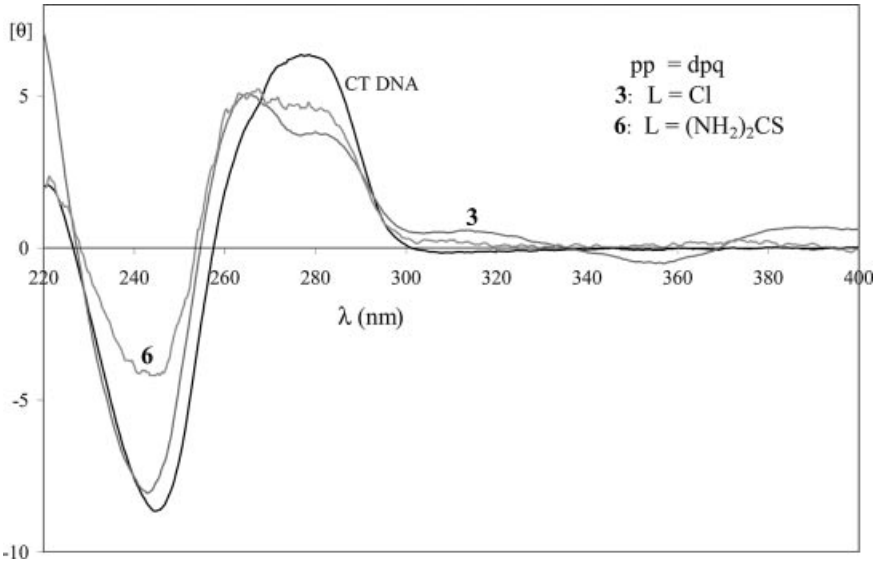

Figure 7. CD spectra of mixtures of **3** and **6** (pp = dpq) with CT DNA (r = 0.1) in a 10 mM phosphate buffer (pH = 7.2) after 24 h incubation.

Both the large increase in $\Delta A/A$ of +63% at 327 nm and the minimal increase in the DNA melting temperature of +2 °C are in accordance with an absence of dppn intercalation for **5**/DNA mixtures under equilibrium conditions. The CD spectrum for such a mixture after 24 h incubation (Figure 8) is closely similar to those registered for the coordinatively bonded phen and tap complexes **1** and **2**. These observations contrast dramatically with other intercalation studies for transition metal complexes, which have established strong intercalative binding for this polypyridyl ligand.[11–13,27] For instance, a binding constant K_b = 7.8×10^4 M^{-1} and site size s of 1.4 have very recently been determined for the complex [Ir(dppn)(ppy)$_2$] (PF_6) (Hppy = 2-phenylpyridine).[27] This K_b value is significantly larger than that of 2.0×10^4 M^{-1} (s = 1.3) obtained for the analogous dppz complex, in accordance with similar findings for rhenium(I) complexes.[11–13] In agreement with the conclusions of Sartorius and Schneider,[9] it seems likely that an enhanced, presumably end-on intercalative binding affinity results from the larger planar surface area of the dppn ligand in comparison to dppz. Intercalative DNA binding has also recently been confirmed for the complexes [Ru(bpy)$_2$(ppip)]$^{2+}$ and [Ru(phen)$_2$(ppip)]$^{2+}$ [ppip = 2-(4′-phenoxyphenyl)imidazo[4,5-*f*][1,10]phenanthroline],[28] whose ppip ligand is even longer than dppn. The apparent lack of intercalation for **5** under equilibrium conditions must, therefore, be attributed to the preferred side-on mode of (η^6-arene)Ru^{II} complexes.[7] It is possible that a kinetically favoured end-on intercalation may lead to the initial dramatic decrease in $\Delta A/A$ of –59% at 327 nm for the **5**/

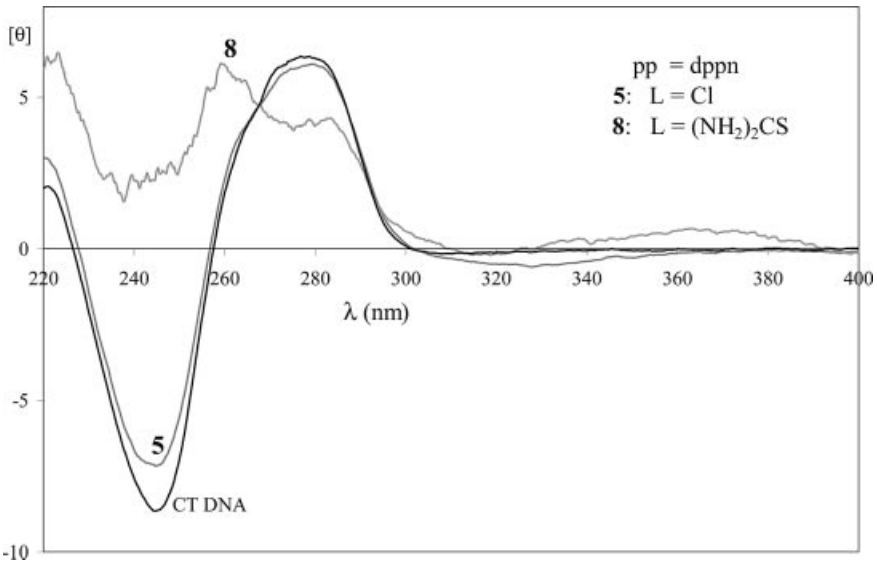

Figure 8. CD spectra of mixtures of **5** and **8** (pp = dppn) with CT DNA (r = 0.1) in a 10 mM phosphate buffer (pH = 7.2) after 24 h incubation.

DNA mixture but that a subsequent rearrangement to a side-on mode with increased base overlap is no longer possible. Support for this line of reasoning is provided by the CD spectrum of the **8**/DNA mixture (Figure 8), for which the stability of the Ru–S (thiourea) bond will be expected to prevent a ligand-substitution reaction and resulting Ru–N (nucleobase) binding. The disappearance of the negative DNA CD band at about 246 nm on the addition of the non-coordinating thiourea complex **8** now implies, in contrast to **5**, DNA damage and complete loss of the original B-helix conformation.

Viscosity Measurements on 3–5

Intercalation of aromatic ligands such as dppz between adjacent nucleobase pairs leads to a lengthening and stiffening of the double helix and these structural changes are reflected in an increase in DNA viscosity.[29,30] The CD spectra of mixtures of the chloro complexes **3**–**5** (pp = dpq, dppz, dppn) with CT DNA suggest that the B conformation of the double helix remains essentially unperturbed in each case, independent of whether the interaction is predominantly intercalative or coordinative. These systems were therefore selected for viscometric titrations and Figure 9 illustrates the dependence of the DNA viscosity on the logarithmic function $\ln(1+r)$ with r = [complex]/[DNA] for complexes **3**–**5**. The slopes of +2.23 and +3.13 for **3** and **4** correlate well with the observed ΔT_m value of +14 and +20 °C and confirm DNA lengthening and thereby intercalation. In contrast, a small decrease in viscosity is observed for the dppn complex **5** in accordance with its small ΔT_m value of +2 °C and the positive $\Delta A/A$ values at equilibrium, which are in accordance with coordinative binding following substitution of the chloride ligand.

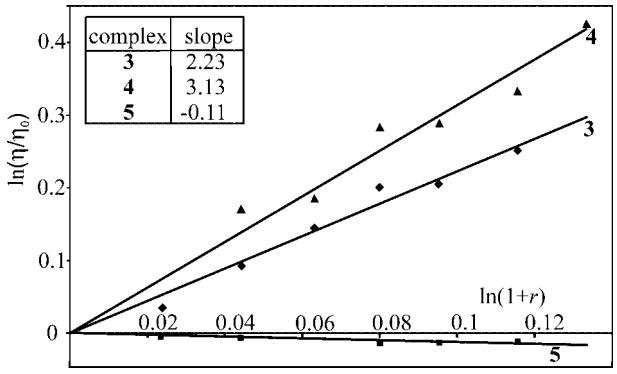

Figure 9. Viscometric titration of sonicated DNA with the complexes **3**–**5** (pp = dpq, dppz, dppn; X = Cl) in a 10 mM phosphate buffer (pH = 7.2): η = reduced viscosity of the DNA solution in the presence of a complex, η_o = the reduced viscosity of the DNA solution without the complex, r = [complex]/[DNA].

It is interesting to compare the DNA binding studies on **3**–**5** with our contrasting recent results for the analogous $(\eta^5\text{-}C_5Me_5)Ir^{III}$ complexes $[(\eta^5\text{-}C_5Me_5)IrCl(pp)](CF_3SO_3)$ (pp = dpq, dppz, dppn),[31] for which chloride substitution will be several orders of magnitude more rapid.[32] Whereas a very small increase is observed for the DNA viscosity (slope = +0.16) on mixing with the $(\eta^5\text{-}C_5Me_5)Ir^{III}$ dpq complex, significant decreases (slopes –1.63 and –1.42) occur for the dppz and dppn complexes. As the ΔT_m values of respectively +2, +7 and +2 °C are modest for the $(\eta^5\text{-}C_5Me_5)Ir^{III}$ complexes and the UV/Vis and CD spectra for their reaction mixtures with CT DNA also provide no evidence for intercalation, it is reasonable to conclude that coordinative Ir–N7 binding to the DNA purine bases must be predominant. The viscosity decreases for the dppz and dppn complexes may be due to kinking or bending of the

double helix[33,34] caused by hydrophobic interactions with the DNA surface and associated polypyridyl stacking.

DNA Binding Parameters for 4

Binding constants K_b in the range 7.3×10^5 to 5.5×10^6 M^{-1} have been determined for least-squares fits to UV/Vis titration data of complexes of the type $[(\eta^6\text{-}C_6Me_6)\text{-}Ru(dppz)(peptide\text{-}\kappa S)]^{n+}$ (n = 2, 3) with CT DNA using the hypochromic absorption shifts at λ_{max} = 364 nm and the non-cooperative non-specific binding model of Bard and Thorp.[35,36] The corresponding site sizes s between 2.3 and 5.1 are in accordance with intercalative binding.[7] It is interesting to compare these parameters with those now obtained for the dppz complexes **4** and **7**. UV/Vis spectra were recorded for buffered 20 μM solutions of **4** and **7** at pH 7.2 following a 60 min incubation with increasing quantities of CT DNA (10–300 μM). An isosbestic point at 399 nm is in each case in accordance with a simple equilibrium distribution between DNA-bound and free $(\eta^6\text{-}C_6Me_6)Ru^{II}$ complex. Figure 10 depicts the least-squares fit to absorbance values recorded for complex **4** at 383 nm, which afforded a K_b value of 2.0(5) 10^6 M^{-1} and a site size s of 1.42(8). The analogous binding parameters for the thiourea complex **7** are 6(3) 10^6 M^{-1} for K_b and 1.55(6) for s. These binding constants are much higher than those of 1.6×10^5 and 1.5×10^5 reported for the monocationic complex cations $[(\eta^6\text{-}C_6Me_6)\text{-}Ru(AcH_{-1}cysOH\text{-}\kappa S)(dppz)]^+$ and $[(\eta^6\text{-}C_6Me_6)Ru(HglyglyH_{-1}cysOH\text{-}\kappa S)(dppz)]^+$ (HcysOH = L-cysteine, HglyOH = glycine) but similar to those of 7.3×10^5–5.5×10^6 M^{-1} previously observed for complex di- and trications of this type (e.g. peptide = AcmetOH, H_2metOMe).[7] The DNA melting temperature increases of 10.4 and 9.4 °C are also much lower for the former monocationic species, whereas the typical ΔT_m values in the range 18.2–18.5 °C for the latter cations are close to that of 20 °C recorded for **4**. These findings suggest that aquation of the original chloride complex $[(\eta^6\text{-}C_6Me_6)RuCl(dppz)]^+$ may take place during the incubation period and that the intercalation data may correspond to the aqua dication $[(\eta^6\text{-}C_6Me_6)Ru(dppz)(H_2O)]^{2+}$. A similar line of reasoning applies to the dpq complex **3**, whose ΔT_m value of 14 °C is close to that of 12 °C recorded for the dications of **6**. The higher K_b value for complex **7** in comparison to **4** may be due to additional hydrogen bonding involving the thiourea ligands.

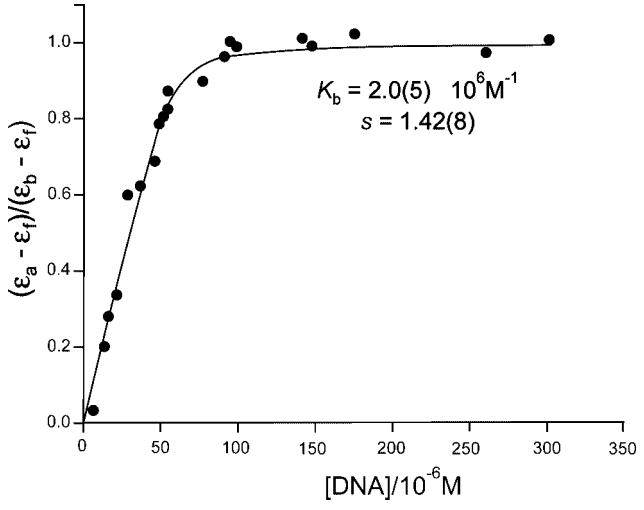

Figure 10. Best least-squares fit to the model of Bard and Thorp[34,35] for the UV/Vis titration data complex **4** with CT DNA.

Cytotoxicity Studies

Table 3 lists the in vitro cytotoxicity of selected $[(\eta^6\text{-}C_6Me_6)Ru^{II}]$ and $[(\eta^5\text{-}C_5Me_5)Ir^{III}]$ complexes against selected human cancer cell lines MCF-7 (breast cancer) and HT-29 (colon cancer). It is apparent for the $[(\eta^6\text{-}C_6Me_6)\text{-}Ru^{II}]$ chloro complexes **3**–**5** that their cytotoxicity is directly correlated to the surface area of the polypyridyl ligand. The IC_{50} values vary in the following order: dppn < dppz < dpq. A similar partial trend (dppn < dppz) can be discerned for the IC_{50} values of the thiourea complexes **7** and **8** towards the HT-29 cell line and to a lesser extent towards MCF-7. Comparison of the observed cytotoxicities for the monocationic and dicationic dppn complexes **5** and **8** suggests that the overall cation charge may also play a role.

On taking our DNA binding studies into account, a number of ways may be proposed in which the polypyridyl ligand could influence the cytotoxicity of this class of compound:

(1) Extending the size of the polypyridyl ligand will confer lipophilic character to the complexes and thereby enhance their uptake into cells. A lower cation charge should likewise favour increased cellular uptake.

(2) Complex recognition and initial kinetically favoured intercalation into the DNA double helix will likewise be enhanced by an increase in the surface area and length of the polypyridyl ligand.

(3) When initial intercalation is followed by substitution of ligand L (or H_2O if aquation has previously taken place), the size of the polypyridyl ligand may influence the degree of distortion of the B DNA conformation caused by coordinative M–N (nucleobase) binding (M = Ru, Ir) or by surface binding.

Inspection of Table 3 indicates that the MCF-7 IC_{50} values for the dppz complexes $[(\eta^6\text{-}C_6Me_6)RuCl(dppz)]^+$ (**4**), $[(\eta^6\text{-}C_6Me_6)Ru(dppz)\{(H_2N)_2CS\}]^{2+}$ (**7**) and $[(\eta^5\text{-}C_5Me_5)\text{-}IrCl(dppz)]^+$ are effectively independent of the nature of the metal or the ligand L. Whereas both **4** and **7** exhibit stable side-on intercalative binding into DNA, relatively rapid Ir–N (nucleobase) coordination is observed for the $(\eta^5\text{-}C_5Me_5)\text{-}Ir^{III}$ complex following initial intercalation.[31] These observations suggest that cell uptake and kinetically favoured DNA intercalation as a rapid recognition process may play the key roles in determining the potency of such organometallic polypyridyl complexes. It is interesting to note, in this respect, that compounds of the type $[(\eta^6\text{-arene})RuCl(en)]^+$ containing polycyclic aromatic coligands have been found to be more potent than the analogous η^6-benzene or η^6-cymene complexes.[15,23] In striking contrast to such (η^6-ar-

Table 3. IC_{50} values (μM)[a] for organometallic polypyridyl (pp) complexes of the types $[(\eta^6\text{-}C_6Me_6)RuL(pp)]^{n+}$ and $[(\eta^6\text{-}C_5Me_5)IrL(pp)]^{n+}$ [L = Cl, n = 1; L = $(NH_2)_2$ CS, n = 2].

Complex	Arene	N,N′-Chelating ligand	L	MCF-7 IC_{50}	HT-29 IC_{50}
(i) Ru^{II} complexes					
3	C_6Me_6	dpq	Cl	11.1 (1.0)	30.3 (5.6)
4	C_6Me_6	dppz	Cl	2.1 (0.6)	2.5 (0.6)
5	C_6Me_6	dppn	Cl	0.13 (0.02)	0.4 (0.1)
7	C_6Me_6	dppz	$(NH_2)_2$ CS	2.5 (0.1)	6.7 (1.2)
8	C_6Me_6	dppn	$(NH_2)_2$ CS	2.1 (0.1)	1.4 (0.4)
(ii) Ir^{III} complexes					
	C_5Me_5	en[37a]	Cl	> 100	
	C_5Me_5	phen[37b]	Cl	> 100	
	C_5Me_5	dppz[31]	Cl	2.3 (0.4)	7.4 (0.9)
	C_5Me_5	dppn[31]	$(NMe_2)_2$CS	0.17 (0.02)	0.41 (0.16)
(iii)	Cisplatin			2.0 (0.3)	7.0 (2.0)

[a] Towards the human cancer cell lines MCF-7 (breast cancer) and HT-29 (colon cancer); the values between brackets represent the standard errors.

ene)Ru^{II} compounds, the IC_{50} values for the polypyridyl complexes of Table 3 appear, however, to be independent of the lability of the M–L bond. The low IC_{50} values for the complex $[(\eta^5\text{-}C_5Me_5)Ir\{(NMe_2)CS\}(dppn)](CF_3SO_3)_2$[31] in comparison to **8** may result from its increased lipophilicity owing to the presence of $(NMe_2)_2CS$ ligands rather than thiourea.

These structure–activity relations suggest that initial DNA recognition and intercalation[38] rather than kinetically controlled coordinative Ru–N(DNA) binding could be of central importance in determining the cytotoxicity of organometallic polypyridyl complexes. It is, therefore, of interest to compare our results with those recently obtained for other metallointercalators. Like the dppz complexes of Table 3, $[Pt(4\text{-}Bu\text{-}ppy)(dppz)](CF_3SO_3)$ is a potent cytotoxic agent and exhibits IC_{50} values some 10 and 40 times lower than cisplatin towards the human cell lines KB-3–1 and KB-V1.[39] In contrast, the dirhodium(II) complexes *cis*-$[Rh_2(\mu\text{-}O_2CCH_3)_2(pp)(O_2CCH_3\text{-}\kappa O)(CH_3OH\text{-}\kappa O)]^+$ (pp = dppz,dppn) are about 4 to 7 times less cytotoxic towards Hs-27 human skin cells than the parent paddlewheel compound *cis*-$[Rh_2(\mu\text{-}O_2CCH_3)_4]$.[40,41] The structure-activity studies on these and other dirhodium complexes are of particular relevance for the present investigation because their IC_{50} values were shown to be related to the lability of the equatorial ligands in the Rh_2 core rather than to the size of the polypyridyl ligand.

Cellular Uptake

In order to evaluate the influence of the cellular uptake on the results of the cytotoxicity experiments we quantified the ruthenium concentration in tumour cells exposed to **3**–**5**, **7** and **8** by atomic absorption spectroscopy. On the basis of the data depicted in Figure 11, it can be concluded that the Ru uptake increases dramatically in the order dpq < dppz < dppn and is much higher for monocationic than for dicationic species with the same polypyridyl ligand, which is in good agreement with the results from the cytotoxicity studies. Accordingly, the highest uptakes of 906.7(1.5) and 1054.7(94.5) ng Ru/mg protein were observed for the monocationic dppn compound **5** with MCF-7 and HT-29 cells, respectively. The dicationic dppn complex **8** exhibited significantly lower cellular ruthenium levels, which were even lower than those found for the monocationic dppz complex **4**. Incubation with the dicationic dppz complex **7** led to decreased cellular ruthenium concentrations in comparison to dppn complex **8** and the monocationic dpq complex **3** was accumulated at the lowest levels with values of only 1.1(1.1) and 11.8(8.5) ng Ru/mg protein being recorded for the cell lines MCF-7 and HT-29. The increase in cellular uptake efficiency with increasing lipophilicity of the ligands is more pronounced for the monocationic series of complexes (**3** << **4** << **5**) than for the dicationic compounds (**7** < **8**). It is apparent that ligand hydrophobicity outweighs the influence of the number of positive charges.

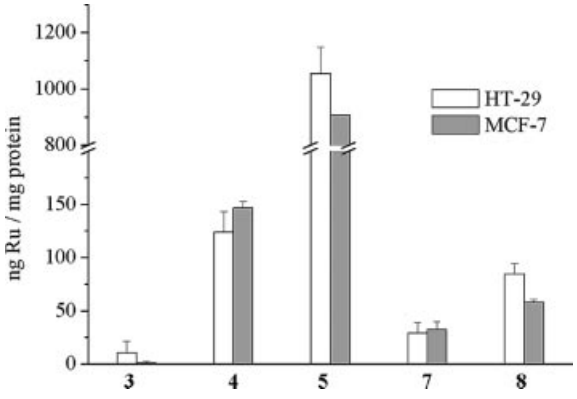

Figure 11. Cellular ruthenium levels in HT-29 and MCF-7 tumour cells after exposure to 10 μM of the complexes for 4 h (n = 2). In some cases the error bars are hidden behind the columns.

The outstanding result is the extraordinarily high uptake of dppn complex **5** which is approximately one order of magnitude higher than the average uptake of the other Ru complexes. Interestingly, this is in good agreement with the significantly lower IC_{50} values of **5** compared to **3**, **4**, **7** and

the second dppn complex **8**. Additional experiments using only 1.0 μM instead of 10 μM solutions of **5** resulted in ruthenium levels [59.1(5.5) ng Ru/mg protein in MCF-7 and 74.5(10.2) ng Ru/mg protein in HT-29 cells] in the range observed for the other compounds at 10 μM. In contrast, the ruthenium content of the samples was found to be below the limit of detection on exposure to 1.0 μM solutions **3**, **4**, **7** and **8**. As compound **3** was barely detectable at 10 μM concentration a higher dosage for this compound was applied for sake of comparison. As expected 100 μM solutions of **3** afforded clearly detectable cellular ruthenium levels of 219.3(80.0) ng Ru/mg protein in MCF-7 and 287.9(43.1) ng Ru/mg protein in HT-29 cells.

Comparison of the cytotoxicity data of Table 3 and the cellular uptake data of Figure 11 indicates that the antiproliferative effects of the complexes were slightly more pronounced in MCF-7 cells than in HT-29 cells (with the exception of **8**) but that the cellular uptake was similar in both tumour cell types. On the basis of distinct cellular parameters (such as cell volume and cell protein content) of MCF-7[42] and HT-29[43] cells, the molar cellular ruthenium concentrations can be estimated from the observed ng/mg values. According to this procedure, 1.0 ng ruthenium per 1.0 mg cell protein correspond to a complex concentration of 1.1 μM in MCF-7 but to 2.0 μM in HT-29 cells. Therefore, the effective molar ruthenium concentrations are higher in HT-29 cells than in MCF-7 cells. Other differences between the two tumour cell types (e.g. the generally faster growth of HT-29 cells) or the intracellular distribution of the complexes will probably play an important role in determining the observed antiproliferative effects. MCF-7 cells are also more sensitive towards the platinum complex cisplatin than HT-29 cells. A decreased activity for cisplatin in colon cancer cells is an established fact, for which resistance phenomena have been made responsible.[44] The uptake of ruthenium indazole complexes such as *trans*-(Hind)[$RuCl_4$-$(ind)_2$] (ind = indazole), KP1019, into HT-29 cells has been reported.[45] In these experiments, a 30 min incubation with 100 μM of the agents resulted in up to 120–160 ng ruthenium being observed per 10^6 cells. Based on the fact that 1.0 mg cell protein of HT-29 cells correspond to approximately 5.6×10^6 cells,[43] the values for the indazole complexes are within the same order of magnitude to those reported in this study, e.g. 188 ng Ru/10^6 cells for 10 μM concentrations of **5** or 51.4 ng Ru/10^6 cells for 100 μM concentrations of **3** in HT-29 cells. It is worth noting, however, that the uptake of **5** was recorded for a tenfold lower complex concentration in comparison to KP1019.

Conclusions

We have demonstrated that the DNA binding of polypyridyl organoruthenium complexes of the types [(η^6-C_6Me_6)-RuCl(pp)](CF_3SO_3) and [(η^6-C_6Me_6)Ru{$(NH_2)_2CS$}(pp)]-(CF_3SO_3)$_2$ is governed by both the size of the polypyridyl ligand and the lability of the Ru–L bond [L = Cl, $(NH_2)_2$-CS]. Whereas stable intercalative binding is observed for the dpq complexes **3**, **4** (L = Cl), **6** and **7** [L = $(NH_2)_2CS$], substitution of the chloride ligand leads to preferred Ru–N (DNA) coordinative binding for both smaller (**1**, phen; **2**, tap) and larger (**5**, dppn) polypyridyl ligands. The significant increase in ΔT_m and DNA viscosity on going from dpq in **3** to dppz in **4** suggest that the latter ligand may offer a close to optimum size for side-on intercalation. In contrast, the cytotoxicity of such compounds appears to be governed mainly by the size of the polypyridyl ligands with IC_{50} values varying in the following order dppn < dppz < dpq. The cellular uptake increases in the order dpq < dppz < dppn and $n = 2 < n = 1$ (n = cation charge) and is in good agreement with the observed IC_{50} values. To the best of our knowledge [(η^5-C_5Me_5)IrCl(dppz)](CF_3SO_3) and [(η^5-C_5Me_5)Ir{$(NMe_2)_2CS$}(dppn)](CF_3SO_3)$_2$ are the first organoiridium(III) complexes with proven in vitro cytotoxicity towards cancer cell lines.

Experimental Section

General: UV/Vis spectra were recorded with an Analytik Jena SPECORD 200 spectrometer and CD spectra with a Jasco J-715 instrument in the range 220–400 nm for 1:10 complex/[DNA] mixtures [complex = 20 μM, DNA concentration in M(nucleotide) = 200 μM] in a 10 mM phosphate buffer at pH 7.2. LSIMS spectra (LSIMS = liquid secondary ion mass spectrometry) were registered for the mass range $m/z < 3000$ with a Fisons VG Autospec employing a caesium ion gun (voltage 17 kV) and 3-nitrobenzyl alcohol as the liquid matrix. A Bruker DRX 400 was employed for the registration of ^1H and ^{13}C NMR spectra with chemical shifts reported as δ values relative to the signal of the deuterated solvent. ^{13}C NMR signals for the CF_3SO_3 anions of **1**–**8** were observed in the range δ = 121.8–122.8 ppm (q) and are not listed for individual complexes. Elemental analyses were performed on a Vario EL of Elementar Analysensysteme GmbH. $RuCl_3 \cdot xH_2O$ and $Ag(CF_3SO_3)$ was obtained from Chempur, 1,10-phenanthroline from J. T. Baker, hexamethylbenzene, thiourea and $(Me_2N)_2CS$ from Acros, and calf thymus DNA (CT DNA) from Sigma. The starting compounds [{(η^6-C_6Me_6)RuCl(μ-Cl)}$_2$],[46] tap,[47] dpq,[48] dppz[49] and dppn[11] were prepared in accordance with literature procedures. All solvents were analytical reagents grade (J. T. Baker) and were dried and distilled before use. [(η^5-C_5Me_5)IrCl(pp)](CF_3SO_3) (pp = phen, dppz) and [(η^5-C_5Me_5)IrCl(en)](CF_3SO_3) were prepared described previously.[31,37]

[(η^6-C_6Me_6)RuCl(phen)](CF_3SO_3) (1): Two equivalents of $Ag(CF_3SO_3)$ (25.7 mg, 0.1 mmol) were added to [{(C_6Me_6)-$RuCl_2$}$_2$] (34.0 mg, 0.05 mmol) and stirred in the dark for 0.5 h in 10 mL acetone. Filtration of the resulting AgCl precipitate and subsequent solvent removal under vacuum afforded [(C_6Me_6)Ru-Cl(acetone)$_2$](CF_3SO_3), which was stirred with the ligand phen (18.0 mg, 0.1 mmol) in CH_3OH/CH_2Cl_2 (1:1, 10 mL) at 55 °C for 2 h. Following volume reduction of the resulting clear solution to 2 mL and addition of CH_3OH (3 mL), the product was precipitated with diethyl ether, washed and dried in vacuo. Yield: 62% (39 mg). $C_{25}H_{26}ClF_3N_2O_3RuS$ (628.1): calcd. C 47.8, H 4.2, N 4.4, S 5.1; found C 47.4, H 4.4, N 4.3, S 5.2. LSIMS: m/z (%) = 593 (2) [M – Cl]$^+$, 479 (100) [M – OTf]$^+$, 444 (10) [M – Cl – OTf]$^+$. ^1H NMR (400 MHz, [D$_6$]DMSO, 25 °C): δ = 2.33 (s, 18 H, CH_3 C_6Me_6), 8.16 (m, 2 H, phen), 8.23 (s, 2 H, phen), 8.80 (dd, 2 H, phen), 9.41 (dd, 2 H, phen) ppm. ^{13}C NMR ([D$_6$]DMSO): δ = 15.8 (CCH_3

C_6Me_6), 97.2 (CCH_3 C_6Me_6), 127.6, 128.8, 131.9, 139.7, 147.2, 154.8 (phen) ppm.

[(η⁶-C_6Me_6)RuCl(tap)](CF_3SO_3) (2): Preparation as for **1** with the ligand tap (18.2 mg, 0.1 mmol). Yield: 70% (44 mg). $C_{23}H_{26}ClF_3N_4O_3RuS$ (630.1): calcd. C 43.9, H 3.8, N 8.9, S 5.1; found C 43.6, H 3.8, N 8.9, S 5.1. LSIMS: *m/z* (%) = 631 (1) [M + H]$^+$, 595 (1) [M – Cl]$^+$, 481 (100) [M – OTf]$^+$, 446 (15) [M – Cl – OTf]$^+$. ^{1}H NMR (400 MHz, [D$_6$]DMSO, 25 °C): δ = 2.31 (s, 18 H, $CH_3C_6Me_6$), 8.61 (s, 2 H, tap), 9.45 (d, 2 H, tap), 9.51 (d, 2 H, tap) ppm. ^{13}C NMR ([D$_6$]DMSO): δ = 16.0 (CCH_3 C_6Me_6), 98.7 (CCH_3 C_6Me_6), 133.7, 146.9, 148.9, 150.9 (tap) ppm.

[(η⁶-C_6Me_6)RuCl(dpq)](CF_3SO_3) (3): Preparation as for **1** with the ligand dpq (23.2 mg, 0.1 mmol). Yield: 46% (31 mg). $C_{27}H_{26}ClF_3N_4O_3RuS$ (680.1): calcd. C 47.7, H 3.9, N 8.2, S 4.7; found C 47.3, H 3.9, N 8.2, S 4.4. LSIMS: *m/z* (%) = 635 (1) [M – Cl]$^+$, 531 (100) [M – OTf]$^+$, 496 (15) [M – Cl – OTf]$^+$. ^{1}H NMR (400 MHz, [D$_6$]DMSO, 25 °C): δ = 2.13 (s, 18 H, CH_3 C_6Me_6), 8.30 (m, 2 H, dpq), 9.33 (s, 2 H, dpq), 9.46 (d, 2 H, dpq), 9.61 (d, 2 H, dpq) ppm. ^{13}C NMR ([D$_6$]DMSO): δ = 15.2 (CCH_3 C_6Me_6), 95.5 (CCH_3 C_6Me_6), 127.6, 128.5, 134.7, 138.9, 146.7, 146.9, 155.0 (dpq) ppm.

[(η⁶-C_6Me_6)RuCl(dppz)](CF_3SO_3) (4): Preparation as for **1** with the ligand dppz (28.2 mg, 0.1 mmol). Yield: 45% (33 mg). $C_{31}H_{28}ClF_3N_4O_3RuS$ (730.2): calcd. C 51.0, H 3.9, N 7.7, S 4.4; found C 50.6, H 3.8, N 7.3, S 4.2. LSIMS: *m/z* (%) = 581 (100) [M – OTf]$^+$, 545 (15) [M – Cl – OTf]$^+$. ^{1}H NMR (400 MHz, [D$_6$]-DMSO, 25 °C): δ = 2.18 (s, 18 H, CH_3 C_6Me_6), 8.19 (m, 2 H, dppz), 8.34 (m, 2 H, dppz) 8.49 (m, 2 H, dppz) 9.46 (dd, 2 H, dppz), 9.71 (dd, 2 H, dppz) ppm. ^{13}C NMR ([D$_6$]DMSO): δ = 17.0 (CCH_3 C_6Me_6), 97.4 (CCH_3 C_6Me_6), 128.9, 130.3, 130.5, 133.6, 136.1, 140.7, 143.0, 149.3, 156.2 (dppz) ppm.

[(η⁶-C_6Me_6)RuCl(dppn)](CF_3SO_3) (5): Preparation as for **1** with the ligand dppn (33.2 mg, 0.1 mmol). Yield: 74% (58 mg). $C_{35}H_{30}ClF_3N_4O_3RuS$ (780.2): calcd. C 53.9, H 3.9, N 7.2, S 4.1; found C 53.9, H 3.8, N 7.1, S 4.2. LSIMS: *m/z* (%) = 631 (100) [M – OTf]$^+$, 596 (10) [M – Cl – OTf]$^+$. ^{1}H NMR (400 MHz, [D$_6$]DMSO, 25 °C): δ = 2.14 (s, 18 H, CH_3 C_6Me_6), 7.73 (m, 2 H, dppn), 8.29 (m, 2 H, dppn), 8.39 (m, 2 H, dppn), 9.16 (s, 2 H, dppn), 9.40 (dd, 2 H, dppn), 9.64 (dd, 2 H, dppn) ppm. ^{13}C NMR ([D$_6$]DMSO): δ = 15.2 (CCH_3 C_6Me_6), 95.5 (CCH_3 C_6Me_6), 127.87, 127.89, 127.91, 128.5, 129.6, 134.5, 135.0, 137.8, 140.0, 148.8, 155.1 (dppn) ppm.

[(η⁶-C_6Me_6)Ru(dpq){$(NH_2)_2CS$}](CF_3SO_3)$_2$ (6): An equivalent of $Ag(CF_3SO_3)$ (25.7 mg, 0.1 mmol) was added to a solution of [{(C_6Me_6)$RuCl_2$}$_2$] (34.0 mg, 0.05 mmol) in 10 mL acetone and stirred in the dark for 0.5 h. Filtration of the precipitate AgCl and subsequent solvent removal under vacuum afforded [(C_6Me_6)Ru-Cl(acetone)$_2$] (CF_3SO_3), which was stirred with the ligand dpq (23 mg, 0.1 mmol) at 55 °C for 2 h. Following solvent removal, the resulting residue of complex 3 was dissolved in 10 mL acetone and treated with a further equivalent of $Ag(CF_3SO_3)$. After stirring in the dark for 0.5 h, filtration of AgCl and solvent removal, the remaining solid was dissolved in 10 mL of a 1:1 CH_3OH/CH_2Cl_2 mixture and treated with thiourea (7.6 mg, 0.1 mmol). The solution was then refluxed for 12 h and subsequently reduced in volume to 2 mL. Following addition of 2 mL of CH_3OH, the product was precipitated by addition of diethyl ether, washed and dried in vacuo. Yield: 44% (38 mg). $C_{29}H_{30}F_6N_6O_6RuS_3$ (869.8): calcd. C 40.0, H 3.5, N 9.7, S 11.1; found C 39.6, H 3.2, N 9.5, S 10.9. LSIMS: *m/z* (%) = 722 (4) [M – OTf]$^+$, 645 (45) [M – OTf – thiourea]$^+$. ^{1}H NMR (400 MHz, [D$_6$]DMSO, 25 °C): δ = 2.10 (s, 18 H, CH_3 C_6Me_6), 7.1 (br., 4 H, thiourea), 8.32 (m, 2 H, dpq), 9.24 (d, 2 H, dpq), 9.37 (s, 2 H, dpq), 9.61 (d, 2 H, dpq) ppm. ^{13}C NMR ([D$_6$]DMSO): δ = 15.4 (CCH_3 C_6Me_6), 97.7 (CCH_3 C_6Me_6), 128.4, 129.1, 134.9, 139.4, 147.0, 147.3, 156.0 (dpq), 174.4 (thiourea) ppm.

[(η⁶-C_6Me_6)Ru(dppz){$(NH_2)_2CS$}](CF_3SO_3)$_2$ (7): Preparation as for **6** with the ligand dppz (29.1 mg, 0.1 mmol). Yield: 63% (58 mg). $C_{33}H_{32}F_6N_6O_6RuS_3$ (919.9): calcd. C 43.1, H 3.5, N 9.1, S 10.5; found C 42.9, H 3.8, N 8.8, S 10.2. LSIMS: *m/z* (%) = 943 (2) [M + Na]$^+$, 771 (12) [M – OTf]$^+$, 695 (7) [M – OTf – thiourea]$^+$, 621 (10) [M – 2OTf]$^+$, 546 (35) [M – 2OTf – thiourea]$^+$. ^{1}H NMR (400 MHz, [D$_6$]DMSO, 25 °C): δ = 2.12 (s, 18 H, CH_3 C_6Me_6), 7.1 (br., 4 H, thiourea), 8.21 (m, 2 H, dppz), 8.32 (m, 2 H, dppz) ppm. 8.53 (m, 2 H, dppz), 9.23 (d, 2 H, dppz), 9.71 (d, 2 H, dppz). ^{13}C NMR ([D$_6$]DMSO): δ = 15.7 (CCH_3), 97.8 (CCH_3), 128.6, 129.7, 129.8, 133.3, 135.2, 140.0, 142.2, 148.5, 156.1 (dppz), 174.4 (thiourea) ppm.

[(η⁶-C_6Me_6)Ru(dppn)] {$(NH_2)_2CS$}(CF_3SO_3)$_2$ (8): Preparation as for **6** with the ligand dppn (32.0 mg, 0.1 mmol). Yield: 47% (46 mg). $C_{37}H_{34}F_6N_6O_6RuS_3$ (970.0): calcd. C 45.8, H 3.5, N 8.7, S 9.9; found C 46.2, H 3.3, N 8.5, S 10.1. LSIMS: *m/z* (%) = 821 (4) [M – OTf]$^+$, 744 (3) [M – 2OTf – thiourea]$^+$ [M – OTf – thiourea]$^+$ 596 (7). ^{1}H NMR (400 MHz, [D$_6$]DMSO, 25 °C): δ = 2.13 (s, 18 H, CH_3 C_6Me_6), 7.2 (br., 4 H, thiourea), 7.82 (m, 2 H, dppn), 8.31 (m, 2 H, dppn), 8.48 (m, 2 H, dppn) 9.19 (m, 2 H, dppn), 9.25 (s, 2 H, dppn), 9.69 (m, 2 H, dppn) ppm. ^{13}C NMR ([D$_6$]DMSO): δ = 15.7 (CCH_3), 97.8 (CCH_3), 128.3, 128.5, 128.8, 129.0, 130.1, 135.0, 135.3, 138.2, 141.1, 149.0, 156.1 (dppn) 174.4 (thiourea) ppm.

X-ray Structural Analysis of 1 and 3: Crystal and refinement data are summarised in Table 1. Intensity data were collected with an Oxford Diffraction Sapphire-CCD diffractometer at 293 K (**1**) and 109 K (**3**) using 1° ω scans and Mo-K_α radiation (λ = 0.71073 Å). The data were corrected for absorption by the Gauss method and solved by direct methods with SHELX97. Refinement against F^2 was performed by SHELXL97[50] with anisotropic temperature factors for non-hydrogen atoms and protons at geometrically calculated positions as riding atoms.

CCDC-635848 to -635849 contain the supplementary crystallographic data for **1** and **3** and may be obtained free of charge at www.ccdc.cam.ac.uk/conts/retrieving.html or from the Cambridge Crystallographic Data Centre, 12 Union Road, Cambridge CB2 1EZ, UK; Fax: +44-1223/336-033; E-mail: deposit@ccdc.cam.ac.uk.

DNA Binding Studies of 1–8: The thermal denaturation temperature T_m of 1:10 complex/DNA mixtures [DNA concentration = M(nucleotide)] were determined in a 10 mM phosphate buffer at pH = 7.2. Melting curves were recorded at 2 °C steps for the wavelength 260 nm with an Analytik Jena SPECORD 200 spectrometer equipped with a Peltier temperature controller. T_m values were calculated by determining the midpoints of melting curves from the first-order derivatives. The experimental ΔT_m values of Table 2 are estimated to be accurate within ±1 °C. Concentrations of CT DNA were determined spectrophotometrically using the molar extinction coefficient ε_{260} = 6600 M^{-1} cm^{-1}.[51]

All electronic absorption titrations were performed at 293 K. After sonication, buffered solutions of CT DNA gave a UV absorbance ration A_{260}/A_{280} of ca. 1.90, indicating that the DNA was sufficiently free of proton.[52] 20 μM solutions of the individual metal complexes were treated with DNA over a range of molarities 20 to 300 μM (nucleotide). All UV/Vis spectra were measured after equilibration, i.e. no further change in the monitored absorbance. Titration curves were constructed from the fractional change in absorbance as a function of DNA concentration according to the

model of Bard and Thorp[35,36] for non-cooperative non specific binding for one type of discrete DNA binding site.

Equation (1) was used to fit the absorption data by least-squares refinement of binding constants (K_b) and site sizes (s) with $b = 1 + K_bC_t + K_b$ [DNA]/2s, where ε_a is the extinction coefficient of the complex in the absence of DNA, ε_b the extinction coefficient of the complex when fully bound to DNA (i.e. no absorption change on further addition of DNA), K_b the equilibrium constant in M^{-1}, C_t the total metal complex concentration, [DNA] the DNA concentration in M(nucleotide) and s the binding site size. Values of ε_b were obtained by extrapolation from the y intercept of plots of $\varepsilon_a/\varepsilon_f$ vs. 1/[DNA]. The K_b and s values of Table 2 are those for the best least-squares fits to the individual UV/Vis titration curves using the program ORIGIN 6.0.

$$(\varepsilon_a - \varepsilon_f)/(\varepsilon_b - \varepsilon_f) = (b - \{b^2 - 2K^2_bC_t[\text{DNA}]/s\}^{1/2})/2K_bC_t \quad (1)$$

Viscosity Measurements: Viscosities for complex/sonicated DNA mixtures were determined using a Cannon–Ubbelhode Semi-micro dilution viscometer (Series No 75, Cannon Instrument Co) held at a constant temperature of 25 °C in a water bath. The viscometer contained 2 mL of 0.4 mM sonicated DNA solution in a 10 mM phosphate buffer (pH = 7.2). 0.2 mM complex solutions also containing sonicated DNA at the same concentration as in the viscometer (0.4 mM) were added in increments of 100 μL from a micropipet. Solutions were passed through filters to remove particulate material prior to use. Reduced viscosities η_O were calculated by literature methods[29] and plotted as $\ln(\eta/\eta_O)$ (η_O = reduced viscosity of the DNA solution in the absence of complex) against $\ln(1+r)$ for rod-like DNA (approximately 600 base pairs).

Cell Culture: MCF-7 breast cancer and HT-29 human colon carcinoma cells were maintained in 10% (v/v) fetal calf serum containing cell culture medium (minimum essential medium eagle supplemented with 2.2 g $NaHCO_3$, 110 mg/L sodium pyruvate and 50 mg/L gentamicin sulfate adjusted to pH 7.4) at 37 °C: 5% CO_2 and passaged twice a week according to standard procedures.

Cytotoxicity Measurements: The antiproliferative effects of the compounds were determined following an established procedure.[53] In short, cells were suspended in cell culture medium (HT-29: 2850 cells/mL, MCF-7: 10000 cells/mL), and 100 μL aliquots thereof were plated in 96 well plates and incubated at 37 °C: 5% CO_2 for 48 h (HT-29) or 72 h (MCF-7). Stock solutions of the compounds in DMSO were freshly prepared and diluted with cell culture medium to the desired concentrations (final DMSO concentration: 0.1% v/v). The medium in the plates was replaced with medium containing the compounds in graded concentrations (six replicates). After further incubation for 72 h (HT-29) or 96 h (MCF-7) the cell biomass was determined by crystal violet staining and the IC_{50} values were determined as those concentrations causing 50% inhibition of cell proliferation. Results were calculated from 2–3 independent experiments.

Cellular Uptake: For cellular uptake studies, cells were grown until at least 70% confluency in 175-cm^2 cell culture flasks. Stock solutions of the complexes in DMSO were freshly prepared and diluted with cell culture medium to the desired concentrations (final DMSO concentration: 0.1% v/v, final complex concentrations: 1.0 and 10 μM). The cell culture medium of the cell culture flasks was replaced with 10 mL of the cell culture medium solutions containing the compounds and the flasks were incubated at 37 °C:5% CO_2 for 4 h. The culture medium was removed, the cell layer washed with 10 mL PBS (phosphate buffered saline pH 7.4), treated with 2–3 mL trypsin solution (0.05% trypsin, 0.02% EDTA in PBS) and incubated for 2 min at 37 °C:5% CO_2 after removal of the trypsin solution. Cells were resuspended in 10 mL PBS and isolated by centrifugation (room temperature, 2000 g, 5 min). The cell pellets were resuspended in 1.0 mL twice distilled water, lysed by use of a sonotrode and appropriately diluted with twice distilled water. The ruthenium content of the samples was determined by AAS (see below) and the protein content by the Bradford method. Results were calculated as ng ruthenium per mg cellular protein from the data obtained in 2 independent experiments.

AAS Measurements: A Vario 6 graphite furnace atomic absorption spectrometer (AnalytikJena AG) was used for ruthenium quantification. Ru was detected at a wavelength of 349.9 nm with a bandpass of 1.2 nm. A deuterium lamp was used for background correction. Standards for calibration purposes were prepared as aqueous dilutions of a commercially available ruthenium standard stock solution [Acros, 1 mg/mL ruthenium in HCl (5%)]. To each 160 μL sample or standard solution 20 μL Triton X-100 (1%) and 40 μL HCl (1 N) were added. A volume of 25 μL thereof was injected into the graphite tubes. Drying, pyrolysis and atomization in the graphite furnace was performed according to the conditions listed in Table 4. The detection limit for the method was 4.8 μg Ru L^{-1}. The mean AUC (area under curve) absorptions of duplicate injections were used throughout the study.

Table 4. Graphite furnace program for AAS measurements.

Step	Temperature [°C]	Ramp [°C/s]	Hold [s]
drying	90	10	40
drying	105	7	30
drying	120	15	20
drying	500	50	30
pyrolysis	900	200	20
AZ (zeroing)	900	0	6
atomisation	2200	maximum	4
tube cleaning	2600	1000	6

Acknowledgments

Financial support of this work in Bochum and Berlin by the Deutsche Forschungsgemeinschaft (DFG) within the research group FOR 630 "Biological function of Organometallic Compounds" is gratefully acknowledged. We are also grateful to Heike Scheffler and Manuela Winter for technical support.

[1] B. Nordén, P. Lincoln, B. Åkerman, E. Tuite, in *Metal Ions in Biological Systems* (Eds.: A. Sigel, H. Sigel) Marcel Dekker, New York, **1996**, *33*, 177.
[2] K. E. Erkkila, D. T. Odom, J. K. Barton, *Chem. Rev.* **1999**, *99*, 2777–2795.
[3] C. Metcalfe, J. A. Thomas, *Chem. Soc. Rev.* **2003**, *32*, 215–224.
[4] D. Herebian, W. S. Sheldrick, *J. Chem. Soc., Dalton Trans.* **2002**, 966–974.
[5] R. Stodt, S. Gençaslan, A. Frodl, C. Schmidt, W. S. Sheldrick, *Inorg. Chim. Acta* **2003**, *355*, 242–253.
[6] S. Gençaslan, W. S. Sheldrick, *Eur. J. Inorg. Chem.* **2005**, 3840–3849.
[7] A. Frodl, D. Herebian, W. S. Sheldrick, *J. Chem. Soc., Dalton Trans.* **2002**, 3664–3673.
[8] T. K. Schoch, J. L. Hubbard, C. R. Zoch, G.-B. Yi, M. Sørlie, *Inorg. Chem.* **1996**, *35*, 4383.
[9] J. Sartorius, H.-J. Schneider, *J. Chem. Soc., Perkin Trans. 2* **1997**, *2*, 2319–2327.
[10] J. Canivet, L. Karmazin-Brelot, G. Süss-Fink, *J. Organomet. Chem.* **2005**, *690*, 3202 –3211.

[11] V. W.-W. Yam, K. K.-W. Lo, K.-K. Cheung, R. Y.-C. Kong, *J. Chem. Soc., Chem. Commun.* **1995**, 1191–1193.
[12] V. W.-W. Yam, K. K.-W. Lo, K.-K. Cheung, R. Y.-C. Kong, *J. Chem. Soc., Dalton Trans.* **1997**, 2067–2072.
[13] K. K.-W. Lo, R. Y.-C. Kong, *Organometallics* **2004**, *23*, 3062–3070.
[14] M. Cusumano, M. L. Di Pietro, A. Giannetto, P. A. Vainiglia, *J. Inorg. Biochem.* **2005**, *99*, 560–565.
[15] Y. W. Yan, M. Melchart, A. Habtemarian, P. J. Sadler, *Chem. Commun.* **2005**, 4764 –4776.
[16] P. J. Dyson, G. Save, *Dalton Trans.* **2006**, 1929–1933.
[17] W. S. Sheldrick, S. Heeb, *Inorg. Chim. Acta* **1990**, *168*, 93–100; S. Heeb, Dissertation, University of Kaiserslautern **1990**, pp110–113.
[18] Y. N. Vashisht Gopal, D. Jayaraju, A. K. Kandapi, *Biochemistry* **1999**, *38*, 4382–4388.
[19] Y. N. Vashisht Gopal, N. Konura, A. K. Kandapi, *Arch. Biochem. Biophys.* **2002**, *401*, 53–62.
[20] L. A. Huxham, E. L. S. Cheu, B. O. Patrick, B. R. James, *Inorg. Chim. Acta* **2003**, *352*, 238–246.
[21] C. S. Allardyce, P. J. Dyson, D. J. Ellis, S. L. Heath, *Chem. Commun.* **2001**, 1396 –1397.
[22] R. E. Morris, R. E. Aird, P. del S. Murdoch, H. M. Chen, J. Cummings, N. D. Hughes, S. Parsons, A. Parkin, G. Boyd, D. I. Jodrell, P. J. Sadler, *J. Med. Chem.* **2001**, *44*, 3616–3621.
[23] A. Habtemarian, M. Melchert, R. Fernandez, S. Parsons, I. D. H. Oswald, A. Prakin, F. P. A. Fabbiani, J. E. Davidson, A. Dawson, R. E. Aird, D. I. Jodrell, P. J. Sadler, *J. Med. Chem.* **2006**, *49*, 6858–6868.
[24] V. Brabec, V. Kleinwächter, J.-L. Butour, N. P. Johnson, *Biophys. Chem.* **1990**, *35*, 129–141.
[25] D. M. Gray, in: *Circular Dichroism and the Conformational Analysis of Biomolecules* (Ed.:G. D. Fasman), Plenum Press, New York. **1996**, 469–500.
[26] W. C. Johnson, in: *Circular Dichroism: Principles and Applications, 2nd Edition* (Eds.: N. Berova, K. Nakanishi, R. W. Woody), VCH Publishers, New York **2000**, 523–540.
[27] K. K.-W. Lo, C.-K. Chung, N. Zhu, *Chem. Eur. J.* **2006**, *12*, 1500–1512.
[28] L.-F. Tan, H. Chao, H. Li, Y.-J. Liu, B. Sun, W. Wei, L.-N. Ji, *J. Inorg. Biochem.* **2005**, *99*, 513–520.
[29] G. Cohen, H. Eisenberg, *Biopolymers* **1966**, *4*, 429–440.
[30] D. Suh, J. B. Chaires, *Bioorg. Med. Chem.* **1995**, *3*, 723–728.
[31] S. Schäfer, W. S. Sheldrick, *J. Organomet. Chem.* **2007**, *692*, 1300–1309.
[32] L. Dadci, H. Elias, U. Frey, A. Hörnig, U. Koelle, A. E. Merbach, H. Paulus, J. S. Schneider, *Inorg. Chem.* **1995**, *34*, 306–315.
[33] A. Raja, V. Rajendrian, P. Uma Masheswari, R. Balamunrugam, C. A. Kilner, M. A. Halcrow, M. Palaniandavar, *J. Inorg. Biochem.* **2005**, *99*, 1717–1732.
[34] B. Selvakumar, V. Rajendrian, P. Uma Mashesuari, H. Stoeckli-Evans, M. Palaniandavar, *J. Inorg. Biochem.* **2006**, *100*, 316–330.
[35] M. T. Carter, M. Rodriguez, A. J. Bard, *J. Am. Chem. Soc.* **1989**, *111*, 8901–8911.
[36] S. R. Smith, G. A. Neyhart, W. A. Karlsbeck, H. H. Thorp, *New J. Chem.* **1994**, *18*, 397–406.
[37] a) M. Scharwitz, T. van Almsick, W. S. Sheldrick, *Acta Crystallogr., Sect. E* **2007**, *63*, m1469–m1470; b) M. Scharwitz, S. Schäfer, T. van Almsick, W. S. Sheldrick, *Acta Crystallogr., Sect. E* **2007**, *63*, m1111–m1113.
[38] J. S. Ren, T. C. Jenkins, J. B. Chaires, *Biochemistry* **2000**, *39*, 8439–8447.
[39] C.-M. Che, M. Yang, K.-H. Wong, H.-L. Chan, W. Lam, *Chem. Eur. J.* **1999**, *5*, 3350 –33346.
[40] A. M. Angeles-Boza, P. M. Bradley, P. K.-L. Fu, S. E. Wicke, J. Bacsa, K. R. Dunbar, C. Turro, *Inorg. Chem.* **2004**, *43*, 8510–8519.
[41] A. M. Angeles-Boza, H. T. Chifotides, J. D. Aguirre, A. Chouai, P. K.-L. Fu, K. R. Dunbar, C. Turro, *J. Med. Chem.* **2006**, *49*, 6841–6847.
[42] R. Gust, B. Schnurr, R. Krauser, G. Bernhardt, M. Koch, B. Schmid, E. Hummel, H. Schoenenberger, *J. Cancer Res. Clin. Oncol.* **1998**, *124*, 585–597.
[43] I. Ott, H. Scheffler, R. Gust, *ChemMedChem* **2007**, *2*, 702–707.
[44] Z. H. Siddik, *Oncogene* **2003**, *22*, 7265–7279.
[45] S. Kapitza, M. Pongratz, M. A. Jakupec, P. Heffeter, W. Berger, L. Lackinger, B. K. Keppler, B. Marian, *J. Cancer Res. Clin. Oncol.* **2005**, *131*, 101–110.
[46] M. A. Bennett, T.-N. Huang, T. W. Matheson, A. K. Smith, *Inorg. Synth.* **1980**, *10*, 74–80.
[47] P. Crochet, B. Demerseman, C. Rocaboy, D. Schleyer, *Organometallics* **1996**, *15*, 3048–3061.
[48] J. G. Collins, A. D. Sleemann, J. R. Aldrich-Wright, I. Greguric, T. W. Hambley, *Inorg. Chem.* **1998**, *37*, 3133–3141.
[49] A. Delgadillo, P. Romo, A. M. Leiva, B. Loeb, *Helv. Chim. Acta* **2003**, *86*, 2110–2120.
[50] G. M. Sheldrick, *SHELXS97 and SHELXL97*, Göttingen, Germany, **1997**.
[51] H.-Q. Liu, T.-C. Cheung, S.-M. Peng, C.-M. Che, *J. Chem. Soc., Chem. Commun.* **1995**, 1787–1788.
[52] J. Marmur, *J. Mol. Biol.* **1961**, *3*, 208–218.
[53] I. Ott, K. Schmidt, B. Kircher, P. Schumacher, T. Wiglenda, R. Gust, *J. Med. Chem.* **2005**, *48*, 622–629.

Received: February 14, 2007
Published Online: May 10, 2007

